Title 論文題目	Erythroid neoplastic cells produced functional erythroferrone to reduce hepcidin in hepatic cells （赤芽球系腫瘍細胞から産生されるエリスロフェロンは肝細胞に作用してヘプシジン産生を低下させる）
Author(s) 著　者	三浦，翔吾
Degree number 学位記番号	甲第 3026 号
Degree name 学位の種別	博士（医学）
Issue Date 学位取得年月日	2018-03-31
Original Article 原著論文	札幌医学雑誌　第 87 巻　第 1 号（平成 31 年 3 月）掲載予定
Doc URL	
DOI	
Resource Version	Author Edition

学位申請論文

Erythroid neoplastic cells produce functional erythroferrone

to reduce hepcidin expression in hepatic cells

腫瘍内科学講座・血液内科学

三浦　翔吾

Erythroid neoplastic cells produce functional erythroferrone to reduce hepcidin expression in hepatic cells

Short title for running head: Production of ERFE in erythroid neoplastic cells

Shogo Miura,[2] Masayoshi Kobune,[1] Shohei Kikuchi,[1,2] Kazuyuki Murase,[1,2] Satoshi Iyama,[1] Koichi Takada,[1,2] Koji Miyanishi,[2] Junji Kato.[2]

[1]Department of Hematology, Sapporo Medical University School of Medicine
[2]Department of Medical Oncology, Sapporo Medical University School of Medicine

Original article

Corresponding author:
Masayoshi Kobune, M.D. and PhD. Department of Hematology, Sapporo Medical University School of Medicine, S-1, W-16, Chuo-Ku, Sapporo, 060-8543, Japan
Telephone number: +81-11-611-2111 (ext. 32540); Fax number: +81-11-612-7987
E-mail Address: mkobune@sapmed.ac.jp

Scientific heading: Myelodysplastic syndrome
Word counts: abstract 200 words, Text 3487 words,
43 References, 2 Tables, 5 Figures
Supplementary files: 2 Supplementary Tables, 3 Supplementary Figures

Abstract

Iron absorption from the gastrointestinal tract was enhanced in a subset of patients with bone marrow failure syndrome (BMFS) exhibiting ineffective erythropoiesis. Duodenal iron absorption was achieved via the ferrous iron transporter, ferroportin, which was downregulated by hepcidin. Recently, a new erythroid regulator, erythroferrone (ERFE), which downregulates hepatic hepcidin production, has been identified. However, how ERFE induces abnormal iron metabolism in BMFS is unclear. In this study, we examined the level of ERFE mRNA during *ex vivo* erythroid differentiation using cord blood CD34+ cells and sodium butylate (SB)-treated K562 cells. Using a public database (GSE58831), we further analyzed whether ERFE could be produced by myelodysplastic syndrome (MDS) cells. ERFE mRNA was increased during normal erythroid differentiation and in SB-treated K562 cells. An analysis of the database indicated that ERFE expression in CD34+bone marrow (BM) MDS cells was higher than that in healthy volunteer (HV)–derived BM CD34+ cells. ERFE expression significantly correlated with the expression of erythropoietin (EPO) receptors (EPO-R). Additionally, the supernatant derived from SB-treated K562 cells reduced the hepcidin level in HepG2 cells in the presence of EPO. These results suggest that EPO-R+ neoplastic cells produce ERFE that may be associated with abnormal iron metabolism via reduced hepcidin.

Background

Multiple genomic mutations in bone marrow (BM) hematopoietic stem/progenitor cells are involved in the development of myelodysplastic syndrome (MDS)[1-3]. Of these, founder gene mutations, including *TET2* and *DNMT3A*, were associated with preclinical clonal hematopoiesis, even that seen in the BM of healthy volunteers (HV)[4, 5]. Subsequently, driver gene mutations were found to determine the disease-specific phenotype and facilitate the clonal evolution of MDS stem/progenitor cells[6]. In this process, the frequency of genomic mutations may be reduced by scavengers of reactive oxygen species (ROS)[7], the nuclear DNA repair system and quiescent cells. Conversely, ROS[8], single cell polymorphisms of the DNA repair system[9], and genotoxic therapy, including chemotherapy and stromal dysfunction[10-12], may accelerate the accumulation of genomic mutations in MDS stem progenitor cells.

Oxidative DNA stress[13, 14] and mitochondrial dysfunction[15] were found to be elevated in patients with transfusion-dependent and transfusion-independent MDS. Moreover, we have previously demonstrated that highly reactive ROS such as hydroxyl radicals (OH·) were also enhanced in BM MDS cells, while the level of 8-hydroxy-2'-deoxyguanosine (8-OHdG) induced by OH· was increased in the genome of MDS-derived mononuclear cells[8]. The production of OH· is known to occur by Fenton or Haber–Weiss reactions using ferrous iron as a cofactor. Iron chelation can reduce the level of labile iron[16, 17] and 8-OHdG in

3

hematopoietic cells[8], and induced hematopoietic recovery[18, 19], resulting in the improvement of the prognosis of MDS patients[20]. Excess iron in the BM could be an accelerator of oxidative DNA damage in patients with MDS, although the precise mechanism on how iron accumulation may occur in patients with MDS is unknown.

Recently, it was shown that the level of serum hepcidin, a direct down-regulator of gastrointestinal iron absorption, was reduced in a proportion of patients with lower risk MDS, such as MDS with ringed sideroblasts (MDS-RS), with single lineage dysplasia (SLD), and MDS-RS with multilineage dysplasia (MLD)[21-23]. Importantly, erythroid regulators such as growth differentiation factor 15 (GDF15), twisted gastrulation protein homolog 1 (TWSG1) and erythroferrone (ERFE), which downregulates hepatic hepcidin production, have recently been identified. Of these, only the expression of ERFE was upregulated after hemorrhage and hemolysis in response to erythropoietin (EPO) stimulation. Moreover, not only GDF15, but ERFE may contribute to suppress the level of hepcidin and enhance gastrointestinal iron absorption to deliver iron into the BM in a mouse model of beta-thalassemia[24, 25]. Based on these findings, we hypothesized that ERFE could be involved in iron delivery to the BM in a subset of patients with MDS via a reduction of hepcidin in hepatocytes.

Here, we evaluated the expression levels of ERFE mRNA in erythroid cells generated from cord blood (CB) CD34+ cells or sodium butylate (SB)–treated K562 cells

4

using an *ex vivo* culture system. We found that the ERFE mRNA level was dramatically

elevated during erythroid differentiation as compared with that in CD34+ cells. We further

analyzed the effect of ERFE on hepcidin expression in hepatocytes and assessed the ERFE

mRNA level in BM CD34+ cells in HV or patients with MDS using public Gene Expression

Omnibus (GEO) data sets (GSE58831).

Materials and Methods

Reagents, cell lines and human CD34+ cells

SB was purchased from Sigma Chemical Corp. (St. Louis, MO). StemPro®-34 (Life

Technologies, Carlsbad, CA) was used as a serum-free medium. Total RNA derived from

human BM CD34+, CB CD34+ and human mesenchymal stromal (MSCs) cells was

purchased from AllCells, LLC (Toronto, Canada). Human BM CD34+ and CB CD34+ cells

were purchased from AllCells, LLC. Human myeloid leukemia cell lines, HEL, HL60 and

U937, were cultured in RPMI1640 containing 10% heat-inactivated fetal calf serum

(FCS; Gibco BRL, Rockville, MD), 2 mM/L L-glutamine, 0.1% penicillin (100 U/mL) and

streptomycin (100 mg/mL). The CD34+ leukemia cell lines, TF-1 and KG-1 (American

Type Culture Collection, Manassa, VA), were cultured in RPMI1640 containing 20%

heat-inactivated FCS, 2 mM/L L-glutamine, 1 mM pyruvate, 0.1% penicillin (100 U/mL)

and streptomycin (100 mg/mL). For the long-term culture of TF-1, 10 U/mL interleukin-3

(IL-3; R&D systems, Minneapolis, MN) was added to the complete medium. The human

erythroleukemia cell line K562 (RCB0027; sensitive to SB) was obtained from RIKEN

BRC CELL BANK (Tsukuba, Japan). K562 cells were cultured in Nutrient Mixture F-12

Ham (HamF12) containing 10% heat-inactivated FCS, and 2 mM/L L-glutamine without

antibiotics. Human embryonic kidney (HEK) 293T cells were cultured in Dulbecco's

Modified Eagle's Medium (DMEM) containing 10% heat-inactivated FCS, 2 mM/L

L-glutamine, 1 mM pyruvate, 0.1% penicillin (100 U/mL) and streptomycin (100 mg/mL).

The diagnostic criteria of MDS in the public database were according to the 2016 revision to

the World Health Organization (WHO) 2016 Classification of myeloid neoplasms and acute

leukemias[26].

Preparation of erythroblasts *ex vivo*.

Primary human MSCs (4×10^5) were plated in a 25-cm^2 flask and cultured until they reached

over 90% confluency. On the first day of coculture, the MSCs were washed five times with

phosphate-buffered saline (PBS) before adding CB CD34+ cells. These CD34+ cells were

seeded on a monolayer of human MSCs in 5 mL of serum-free StemPro®-34 medium (Life

Technologies) supplemented with 50 ng/mL thrombopoietin (TPO), 10 ng/mL human stem

cell factor (SCF) and 50 ng/mL human Fms-related tyrosine kinase 3 ligand (FLT3LG; all

R&D Systems), and maintained at 37°C under 5% CO_2. All hematopoietic cells that had

been cocultured with MSCs were collected as previously described[27]. Erythroid

differentiation was carried out in a serum-free liquid culture system without a human stromal

layer. In the first step, hematopoietic progenitor cells at 1×10^6/mL were suspended in

erythroid induction medium, which consisted of StemPro®-34 medium with 10 ng/mL SCF, 4

U/mL erythropoietin (EPO), 100 U/mL IL-3, 20 ng/mL insulin-like growth factor (IGF)-1 (R&D

Systems) and 500 μg/mL iron-saturated transferrin (Sigma Chemical Corp.). The cells were

incubated in a humidified atmosphere of 5% CO_2 at 37°C for 7 days. In the second step,

progenitor cells that had been induced toward the erythroid lineage were suspended in

erythroid maturation medium, which consisted of erythroid induction medium that did not

contain IL-3 and SCF. The cells were incubated at 3×10^6/mL in a humidified atmosphere of

5% CO_2 for 7 days[28].

Production of human recombinant ERFE

A Myc-DKK–tagged human ERFE plasmid (RC237678; ERFE plasmid) was purchased from

OriGene Technologies, Inc. (Rockville, MD). HEK293T cells were seeded on 10-cm tissue

culture dishes. When cells reached 90% confluency, 14 μg of ERFE plasmids were

transfected using lipofectamine™ LTX Reagent with PLUS Reagent according to the manufacturer's instructions. Ninety-six hours after transfection, the supernatant was passed through a 0.45 filter (Merck Millipore, Tokyo, Japan) and stored before use. ERFE protein was confirmed by immunoblot analysis using anti-DDK (FLAG) monoclonal antibody (Clone OTI4C5, OriGene).

Differentiation of K562 cells into dysplastic erythroid cells in the presence of SB

For experiments, cells were seeded at a density of 4×10^5 cells/4 mL in 35-mm dishes and cultured for 0 – 4 days in the presence or absence of 1.0 mM SB, with or without 4 U/mL EPO. The differentiation of erythroid cells was confirmed by morphological change (May–Giemsa staining) and flow cytometric analysis as described below.

Analysis of mRNA

For reverse transcription, total RNA was prepared from cells using Trizol reagent according to the manufacturer's instructions (Invitrogen, Waltham, MA). Total RNA (1 μg) was reverse transcribed with a SuperScript® VILO™ cDNA Synthesis Kit (Invitrogen) for Taqman PCR or SYBR® Green PCR. Taqman Assays IDs (Applied Biosystems, Foster City, CA) and Real-time SYBR® Green PCR, primer set IDs are shown in Supplementary Tables 1 and 2.

Quantitative real-time (qRT)–PCR was performed in triplicate using the ABI PRISM®7300

Sequence Detection System (PE Applied Biosystems) in a 50 μL reaction volume. Relative

gene expression was calculated as the signal ratio of target gene (*FAM*) to S18 cDNA.

Immunophenotyping of *ex vivo* cultured hematopoietic cells

Aliquots of cells were stained with fluorescein isothiocyanate (FITC)– and/or phycoerythrin

(PE)-conjugated monoclonal antibodies, including isotype control antibodies (BD

Biosciences, San Jose, CA). Cells were incubated with FITC-conjugated

anti-erythropoietin receptor (EPO-R; R&D Systems), PE-conjugated anti-glycophorin A

(GPA) (Immunotech), or allophycocyanin (APC)-conjugated anti-CD34 (BD Biosciences,

Tokyo, Japan) antibodies at 4°C for 60 min, and then washed twice with PBS containing

0.1% BSA. The cells were analyzed by flow cytometric analysis using FACSCanto (Becton

Dickinson, Mountain View, CA) and dead cells were gated out by propidium iodide (PI)

staining.

Analysis of public database

For analysis of CD34+ cells, Gene Expression Omnibus (GEO) data sets (GSE58831) of

gene expression were downloaded and quintiles normalized using an affy Bioconductor

package (R commander version 3.4.1). Since this data set included acute leukemia (AML, n=7), chronic myelomonocytic leukemia (CMML, n=7), MDS with excess blasts (MDS-EB) with an unknown percentage of blasts (n=14) and unknown diagnosis (n=1), the data for these diseases was excluded by dplyr package (R commander) to form a new database (data set MDS1). Data set MDS1 also included a specific category of MDS, such as MDS-RS-SLD carrying an *SF3B1* mutation and MDS with isolated del(5q), which exhibited a specific phenotype of MDS. Hence, we also excluded cases of MDS-RS-SLD (n=20) and MDS with an isolated del(5q) (n=6) by dplyr package (R commander) to make up data sets of MDS2 consisting of HV (n=17), MDS-SLD (n=13), MDS-MLD (n=27), MDS-RS-MLD (n=22), MDS-EB-1 (n=14) and MDS-EB-2 (n=28) for further analysis.

Statistical analysis

Each data set was first evaluated for the normality of distribution by the Komolgorov–Smirnov test to decide whether a non-parametric rank–based or a parametric analysis should be used. The significance of differences between groups was assessed by one-way ANOVA test with a post-hoc Tukey Honestly Significant Difference Test. Results are expressed as the mean ± standard deviation (SD). The significance of differences was assessed by either the Student's *t*-test or the Mann-Whitney *U*–test, and a *p*-value < 0.05

was considered as statistically significant. All statistical analyses were performed with R commander or EZR (Easy R) software, which is a graphical user interface for R[29].

Results

The mRNA expression of erythroid regulators in erythroblasts and leukemic cell lines

We first investigated the expression level of ERFE, GDF15 and TWSG1 in *ex vivo* cultured erythroblasts and leukemic cell lines to obtain insights into the specificity of erythroid expression. Erythroid cells were produced *ex vivo* from CB CD34+ cells in the presence of SCF, IL-3 and EPO as previously described (Fig. 1a)[28, 30, 31]. The hemoglobin (Hb) content per cell (mean corpuscular hemoglobin, MCH) was significantly elevated during culture for 14 days (Fig. 1b; $p < 0.05$). Remarkably, ERFE mRNA was approximately a thousand-fold higher 14 days after the EPO stimulation of erythroblasts (Fig. 1c; $p<0.01$). The expression of GDF15 mRNA was thirty-fold higher in erythroid cells 14 days after EPO stimulation (Supplementary Fig. 1; $p < 0.01$). Conversely, TWSG1 mRNA expression during erythroid differentiation was comparable with that of leukemic cell lines such as TF-1, KG-1 and K562 (Supplementary Fig. 2; $p < 0.01$). Based on these findings, we focused on ERFE and further examined its expression in MDS.

Analysis of ERFE mRNA levels in CD34+ MDS cells using a GEO database

To check the gene expression of ERFE in CD34+ MDS cells, we employed a subset of a public GEO database (GSE58831) in which the transcriptomes in CD34+ MDS and CD34+ normal BM cells were analyzed. ERFE gene expression in CD34+ MDS cells was significantly higher than that in CD34+ cells derived from HV (Fig. 2a; $p < 0.000005$). In the

WHO classification of MDS, ERFE expression in CD34+ cells derived from MDS-RS-SLD was higher than that in other subgroups of MDS (data not shown). Considering the involvement of ringed sideroblasts that correlated with the *SF3B1* mutation, data set MDS1, including MDS-RS-SLD and MDS with isolated del(5q), was further analyzed. As expected, multiple regression analysis revealed that only the *SF3B1* mutation positively correlated with a higher expression of ERFE mRNA (Table 1). Moreover, we selected highly expressed genes in MDS from data set MDS1 as compared with those expressed in HV, and subsequently analyzed the statistical correlation between ERFE and these genes using stepwise regression analysis. As a result, several genes, including *ALAS2* and *EPO-R*, significantly and positively correlated with ERFE (Table 2). Since the result of MDS-RS-SLD with a *SF3B1* mutation was extraordinary, we subsequently utilized the MDS2 data set without specific subtypes of MDS, including MDS-RS-SLD, and MDS with isolated del(5q). For the WHO classification of data set MDS2, ERFE expression in CD34+ cells derived from MDS-RS-MLD without an *SF3B1* mutation was significantly higher than that of other subgroups of MDS (Fig. 2b; $p < 0.001$, HV vs. MDS-RS-MLD; $p < 0.00005$, HV vs. MDS). The expression of EPO-R in CD34+ MDS cells was significantly higher than that in CD34+ cells derived from HV (Fig 2c; $p < 0.05$). For data set MDS2, EPO-R mRNA expression in CD34+ cells derived from MDS-RS-MLD was significantly higher than that in other subgroups of MDS (Fig. 2d). Of these, EPO-R mRNA levels significantly correlated with ERFE mRNA levels (Fig. 3; $p < 0.01$). These results suggested that ERFE mRNA expression may be associated with the *SF3B1* mutation, the presence of ringed sideroblasts and EPO-R mRNA expression in erythroid neoplastic cells.

The effect of ERFE on hepatocyte cell lines

ERFE is thought to mediate hepcidin suppression during stress erythropoiesis. However, it remains unclear whether ERFE directly affects hepatocytes to reduce the hepcidin level. Since ERFE is secreted as a trimeric complex[32, 33], a plasmid with the *ERFE* gene was transfected into HEK293T cells to produce ERFE protein. Mock-transduced conditioned medium (Control CM) and ERFE plasmid–transduced CM (ERFE CM) were collected before analyses (Fig. 4a). The production of DKK-tagged ERFE protein was confirmed using anti-DKK antibody (data not shown). We evaluated the effect of ERFE on the production of hepcidin from hepatoma cell lines, including HuH7 and HepG2, using control and ERFE CM. Unexpectedly, HuH7 did not response to ERFE CM and the expression level of hepcidin mRNA remained low, even before exposure to ERFE CM (Fig. 4b, upper panel). In clear contrast, HepG2 cells responded to ERFE CM in a significant, dose-dependent manner (Fig. 4b, lower panel; $p < 0.05$). Therefore, we decided to use HepG2 for our next experiments.

The differentiation of K562 cells into dysplastic erythroid cells and effect of supernatant on hepatocytes

Finally, we evaluated whether ERFE derived from dysplastic erythroid cells affected hepcidin expression in hepatocytes. For this experiment, HepG2 cells were used as hepatocyte surrogates. K562 cells, which were confirmed to be sensitive to SB, were used in these experiments. K562 cells showed homogeneous blastic cells before SB treatment (Fig. 5a, left panel). Two days after SB treatment, some of the K562 cells had differentiated into basophilic erythroblasts and exhibited differences in size (Fig. 5a, middle panel). Four days after SB treatment, K562 cells had further differentiated into polychromatic erythroblasts; however, some exhibited dysplasia with multiple nuclei (Fig. 5a, right panel). Flow cytometric analysis indicated that K562 cells before SB treatment and expressing

CD235a (glycophorin A) could be divided into two groups (Fig. 5b, upper panel). One group did not show expression of CD235a while the other demonstrated low expression of CD235a. During SB treatment, CD235a expression was gradually elevated and all SB-treated K562 cells exhibited high CD235a expression. The expression level of CD71 and EPO-R was not significantly changed after SB treatment (Fig. 5b, lower panel). These results suggested that K562 cells showed an erythroid phenotype, even before SB treatment, and that SB-treated K562 cells differentiated toward mature erythroblasts with dysplasia. We next assessed the expression of ERFE in SB-treated K562 cells in the presence or absence of EPO. The ERFE level before SB treatment remained low. ERFE expression in K562 cells was elevated in response to EPO probably because K562 cells expressed EPO-R (data not shown). Subsequently, we evaluated the effect of CM derived from K562 cells on hepcidin production in HepG2 cells (Fig. 5c). The reduction in hepcidin was observed after exposure of supernatant derived from SB-treated K562 cells in the presence of EPO ($p < 0.05$). These results indicated that ERFE was highly expressed in response to EPO in dysplastic erythroid cells and that ERFE functionally affected the hepcidin level in hepatocytes.

Discussion

In the present study, we found that ERFE production is increased during *ex vivo* erythroid differentiation from CB CD34+ cells in the presence of EPO. Moreover, ERFE was highly produced by CD34+ MDS cells as well as dysplastic erythroid cells derived from SB-treated K562 cells in response to EPO. Furthermore, the ERFE from dysplastic erythroid cells functionally reduced the hepcidin level in the hepatocyte cell line, HepG2.

Previously, it was found that excess tissue iron increased in the presence of

ineffective erythropoiesis by analysis using iron radioisotopes, tissue iron staining and Magnetic Resonance Imaging (MRI)[34]. However, it was unclear whether the elevation of body storage iron could be attributed to increased gastrointestinal iron absorption[34, 35]. However, a substitute marker of iron overload such as serum ferritin and MRI R2 clearly showed hepatic iron accumulation even in transfusion-independent MDS patients[36, 37], suggesting that iron accumulation in MDS patients is not always dependent upon transfusion-associated iron loading. Consistent with these reports, the analysis of GEO data sets (GSE58831) indicated that a proportion of MDS patients, irrespective of WHO category, exhibited hyperferritinemia (Supplementary Fig. 3). These results suggested that certain molecular mechanisms may be implicated in excess tissue iron in patients with MDS[25]. In these analyses, we focused on the newly-identified erythroid regulator, ERFE, and found that ERFE mRNA was elevated in the CD34+ cells of MDS patients. These results suggest that ERFE is involved in abnormal iron metabolism in patients with MDS.

Next, we investigated the relationship between the ERFE level and the WHO category of MDS. In this study, as shown in Figure 2, the level of ERFE was higher in MDS-RS-MLD as compared with others. When we analyzed the relationship between gene mutation and the ERFE level, the presence of an *SF3B1* mutation significantly correlated with ERFE expression (Table 1). Regarding the analysis of GEO data sets (GSE58831), ERFE expression in CD34+ cells derived from transfusion-independent MDS and the average level of serum ferritin were the highest in MDS-RS-SLD patients (Supplementary Fig. 3). These results were consistent with a previous report showing that patients with MDS-RS-SLD exhibited a high serum ferritin level[38]. Importantly, the level of hepcidin, which down-regulates the ferroportin transporter in duodenum, was reduced in patients with MDS-RS-SLD[23], and GDF15 did not correlate with the hepcidin level[23]. These results seem

15

to support our findings and results from GEO data sets (GSE58831) showing that the iron regulator, ERFE, was significantly elevated in the BM of MDS patients, especially those with MDS-RS-SLD and MDS-RS-MLD[23]. Thus, ERFE may contribute to reducing hepatic hepcidin production in MDS patients.

In the present study, we provide data set MDS2, in which specific clinical entities of MDS such as MDS-RS-SLD and MDS with isolated del(5q) were excluded from GEO data sets (GSE58831), and analyzed for gene expression in MDS in more detail. By multiple linear regression analysis, the level of ERFE in CD34+ MDS cells most strongly correlated with that of EPO-R (Fig. 3 and Table 2). In this regard, ERFE mRNA in erythroid cells derived from human BM could be highly upregulated in response to EPO[39]. Further, blockade of JAK2/STAT5 signaling resulted in a reduction of the ERFE level[39]. Based on these findings, we hypothesized that the increased production of ERFE in dysplastic erythroid cells could be achieved in response to EPO via EPO-R. In fact, in this study, the level of ERFE mRNA in SB-treated K562 cells as well as erythroid cells differentiated from CB CD34+ cells were significantly elevated in the presence of EPO as compared with that in the absence of EPO. These findings suggested that erythroid dysplastic cells expressing EPO-R could be a major source of ERFE production.

In conclusion, ERFE expression in BM CD34+ cells in patients with MDS is higher than in normal BM. ERFE expression is enhanced in erythroid dysplastic cells in response to EPO. The produced ERFE could reduce hepcidin level in hepatocytes. Thus, ERFE expression in EPO-R+ erythroid dysplastic cells may contribute to aberrant iron metabolism.

Acknowledgements

Author Contributions

Contribution: SM contributed to most experiments. MK designed experiments, analyzed results from the GEO database and drafted the paper. SK established the coculture system of primary myeloid cells. KM conducted MG staining of K562. SI, KT and KM helped with the statistical analysis of the data. JK edited the final version of this paper.

References

1. Kwok B, Hall JM, Witte JS, Xu Y, Reddy P, Lin K*, et al.* MDS-associated somatic mutations and clonal hematopoiesis are common in idiopathic cytopenias of undetermined significance. *Blood*; **126:** 2355-2361 (2015).

2. Colla S, Ong DS, Ogoti Y, Marchesini M, Mistry NA, Clise-Dwyer K*, et al.* Telomere dysfunction drives aberrant hematopoietic differentiation and myelodysplastic syndrome. *Cancer Cell*; **27:** 644-657 (2015).

3. Lee SC, Dvinge H, Kim E, Cho H, Micol JB, Chung YR*, et al.* Modulation of splicing catalysis for therapeutic targeting of leukemia with mutations in genes encoding spliceosomal proteins. *Nat Med*; **22:** 672-678 (2016).

4. Cargo CA, Rowbotham N, Evans PA, Barrans SL, Bowen DT, Crouch S*, et al.* Targeted sequencing identifies patients with preclinical MDS at high risk of disease progression. *Blood*; **126:** 2362-2365 (2015).

5. Steensma DP, Bejar R, Jaiswal S, Lindsley RC, Sekeres MA, Hasserjian RP*, et al.* Clonal hematopoiesis of indeterminate potential and its distinction from myelodysplastic syndromes. *Blood*; **126:** 9-16 (2015).

6. Mossner M, Jann JC, Wittig J, Nolte F, Fey S, Nowak V*, et al.* Mutational hierarchies in myelodysplastic syndromes dynamically adapt and evolve upon therapy response and failure. *Blood***:**   (2016).

7. Yan F, Yang WK, Li XY, Lin TT, Lun YN, Lin F*, et al.* A trifunctional enzyme with glutathione S-transferase, glutathione peroxidase and superoxide dismutase activity. *Biochim Biophys Acta*; **1780:** 869-872 (2008).

8. Kikuchi S, Kobune M, Iyama S, Sato T, Murase K, Kawano Y*, et al.* Improvement of iron-mediated oxidative DNA damage in patients with transfusion-dependent myelodysplastic syndrome by treatment with deferasirox. *Free Radic Biol Med*; **53:** 643-648 (2012).

9. Dubois J, Etienne G, Laroche-Clary A, Lascaux A, Bidet A, Lippert E*, et al.* Identification of methylguanine methyltransferase polymorphisms as genetic markers of individual susceptibility to therapy-related myeloid neoplasms. *Eur J Cancer*; **50:** 418-424 (2014).

10. Raaijmakers MH, Mukherjee S, Guo S, Zhang S, Kobayashi T, Schoonmaker JA*, et al.* Bone progenitor dysfunction induces myelodysplasia and secondary leukaemia. *Nature*; **464:** 852-857 (2010).

11. Mendez-Ferrer S, Michurina TV, Ferraro F, Mazloom AR, Macarthur BD, Lira SA*, et al.* Mesenchymal and haematopoietic stem cells form a unique bone marrow niche. *Nature*;

466: 829-834 (2010).

12. Balderman SR, Li AJ, Hoffman CM, Frisch BJ, Goodman AN, LaMere MW*, et al.* Targeting of the bone marrow microenvironment improves outcome in a murine model of myelodysplastic syndrome. *Blood*; **127:** 616-625 (2016).

13. Saigo K, Takenokuchi M, Hiramatsu Y, Tada H, Hishita T, Takata M*, et al.* Oxidative stress levels in myelodysplastic syndrome patients: their relationship to serum ferritin and haemoglobin values. *J Int Med Res*; **39:** 1941-1945 (2011).

14. Guida M, Maraldi T, Beretti F, Follo MY, Manzoli L, De Pol A. Nuclear Nox4-derived reactive oxygen species in myelodysplastic syndromes. *Biomed Res Int*; **2014:** 456937 (2014).

15. Goncalves AC, Cortesao E, Oliveiros B, Alves V, Espadana AI, Rito L*, et al.* Oxidative stress and mitochondrial dysfunction play a role in myelodysplastic syndrome development, diagnosis, and prognosis: A pilot study. *Free Radic Res*; **49:** 1081-1094 (2015).

16. Kim IH, Moon JH, Lim SN, Sohn SK, Kim HG, Lee GW*, et al.* Efficacy and safety of deferasirox estimated by serum ferritin and labile plasma iron levels in patients with aplastic anemia, myelodysplastic syndrome, or acute myeloid leukemia with transfusional iron overload. *Transfusion*; **55:** 1613-1620 (2015).

17. Porter JB, El-Alfy M, Viprakasit V, Giraudier S, Chan LL, Lai Y*, et al.* Utility of labile plasma iron and transferrin saturation in addition to serum ferritin as iron overload markers in different underlying anemias before and after deferasirox treatment. *Eur J Haematol*; **96:** 19-26 (2016).

18. Hartmann J, Braulke F, Sinzig U, Wulf G, Maas JH, Konietschke F*, et al.* Iron overload impairs proliferation of erythroid progenitors cells (BFU-E) from patients with myelodysplastic syndromes. *Leuk Res*; **37:** 327-332 (2013).

19. Visani G, Guiducci B, Giardini C, Loscocco F, Ricciardi T, Isidori A. Deferasirox improves hematopoiesis after allogeneic hematopoietic SCT. *Bone Marrow Transplant*; **49:** 585-587 (2014).

20. Lyons RM, Marek BJ, Paley C, Esposito J, Garbo L, DiBella N*, et al.* Comparison of 24-month outcomes in chelated and non-chelated lower-risk patients with myelodysplastic syndromes in a prospective registry. *Leuk Res*; **38:** 149-154 (2014).

21. Zipperer E, Post JG, Herkert M, Kundgen A, Fox F, Haas R*, et al.* Serum hepcidin measured with an improved ELISA correlates with parameters of iron metabolism in patients with myelodysplastic syndrome. *Ann Hematol*; **92:** 1617-1623 (2013).

22. Gu S, Song X, Zhao Y, Guo J, Fei C, Xu F*, et al.* The evaluation of iron overload through hepcidin level and its related factors in myelodysplastic syndromes. *Hematology*; **18:**

286-294 (2013).

23.   Santini V, Girelli D, Sanna A, Martinelli N, Duca L, Campostrini N*, et al.* Hepcidin levels and their determinants in different types of myelodysplastic syndromes. *PLoS One*; **6:** e23109 (2011).

24.   Kautz L, Jung G, Du X, Gabayan V, Chapman J, Nasoff M*, et al.* Erythroferrone contributes to hepcidin suppression and iron overload in a mouse model of beta-thalassemia. *Blood*; **126:** 2031-2037 (2015).

25.   Tanno T, Bhanu NV, Oneal PA, Goh SH, Staker P, Lee YT*, et al.* High levels of GDF15 in thalassemia suppress expression of the iron regulatory protein hepcidin. *Nat Med*; **13:** 1096-1101 (2007).

26.   Arber DA, Orazi A, Hasserjian R, Thiele J, Borowitz MJ, Le Beau MM*, et al.* The 2016 revision to the World Health Organization classification of myeloid neoplasms and acute leukemia. *Blood*; **127:** 2391-2405 (2016).

27.   Kobune M, Kawano Y, Ito Y, Chiba H, Nakamura K, Tsuda H*, et al.* Telomerized human multipotent mesenchymal cells can differentiate into hematopoietic and cobblestone area-supporting cells. *Exp Hematol*; **31:** 715-722 (2003).

28.   Kobune M, Kawano Y, Kato J, Ito Y, Chiba H, Nakamura K*, et al.* Expansion of CD34+ cells on telomerized human stromal cells without losing erythroid-differentiation potential in a serum-free condition. *Int J Hematol*; **81:** 18-25 (2005).

29.   Kanda Y. Investigation of the freely available easy-to-use software 'EZR' for medical statistics. *Bone Marrow Transplant*; **48:** 452-458 (2013).

30.   Horiguchi H, Kobune M, Kikuchi S, Yoshida M, Murata M, Murase K*, et al.* Extracellular vesicle miR-7977 is involved in hematopoietic dysfunction of mesenchymal stromal cells via poly(rC) binding protein 1 reduction in myeloid neoplasms. *Haematologica***:**   (2016).

31.   Fujimi A, Matsunaga T, Kobune M, Kawano Y, Nagaya T, Tanaka I*, et al.* Ex vivo large-scale generation of human red blood cells from cord blood CD34+ cells by co-culturing with macrophages. *Int J Hematol*; **87:** 339-350 (2008).

32.   Seldin MM, Peterson JM, Byerly MS, Wei Z, Wong GW. Myonectin (CTRP15), a novel myokine that links skeletal muscle to systemic lipid homeostasis. *J Biol Chem*; **287:** 11968-11980 (2012).

33.   Kautz L, Jung G, Nemeth E, Ganz T. Erythroferrone contributes to recovery from anemia of inflammation. *Blood*; **124:** 2569-2574 (2014).

34.   Marx JJ. Normal iron absorption and decreased red cell iron uptake in the aged. *Blood*; **53:** 204-211 (1979).

35.   Bennett JM, Catovsky D, Daniel MT, Flandrin G, Galton DA, Gralnick HR*, et al.* Proposals for the classification of the myelodysplastic syndromes. *Br J Haematol*; **51:**

189-199 (1982).

36. Kikuchi S, Kobune M, Iyama S, Sato T, Murase K, Kawano Y*, et al.* Prognostic significance of serum ferritin level at diagnosis in myelodysplastic syndrome. *Int J Hematol*; **95:** 527-534 (2012).

37. Gattermann N, Rachmilewitz EA. Iron overload in MDS-pathophysiology, diagnosis, and complications. *Ann Hematol*; **90:** 1-10 (2011).

38. Park S, Sapena R, Kelaidi C, Vassilieff D, Bordessoule D, Stamatoullas A*, et al.* Ferritin level at diagnosis is not correlated with poorer survival in non RBC transfusion dependent lower risk de novo MDS. *Leuk Res*; **35:** 1530-1533 (2011).

39. Kautz L, Jung G, Valore EV, Rivella S, Nemeth E, Ganz T. Identification of erythroferrone as an erythroid regulator of iron metabolism. *Nat Genet*; **46:** 678-684 (2014).

Figure legends

Fig. 1 Differentiation of erythroids from bone marrow CD34+ cells that had expanded above bone marrow mesenchymal stromal cells and expression levels of ERFE mRNA. a Flow cytometric analysis of hematopoietic cells after expansion (day 0), and after days 7 and 14 of erythroid induction in the presence of erythropoietin (EPO). Hematopoietic cells were immunolabeled with fluorescein isothiocyanate (FITC)–conjugated CD71 and phycoerythrin (PE)-conjugated CD235a antibodies on the indicated days. **b** Comparison of the hemoglobin (Hb) content per cell (mean corpuscular hemoglobin; MCH) on days 0, 7 and 14 after the start of erythroid differentiation. Each bar represents the mean ± standard deviation (S.D.) in 10^6 hematopoietic cells. $*p <$ 0.05 vs. day 0 in the respective group. **c** Analysis of the expression of erythroid regulators in erythroid cells and leukemic cell lines. The expression levels of erythroferrone (ERFE) mRNA were examined by Taqman quantitative real-time (qRT)–PCR). Results are expressed as means ± SD. $*p < 0.05$, $**p < 0.01$ vs. day 0 in the respective group.

Fig. 2 Analysis of ERFE and EPO-R mRNA, and hematological parameters using a public database. The data set MDS2 (subclass of GSE58831), consisting of MDS-SLD, MDS-MLD, MDS-RS-ML D, MDS-EB-1 and MDS-EB-2, was used for these analyses. **a** The level of ERFE mRNA in patients with myelodysplastic syndrome (MDS; n=104) was compared with that in healthy volunteers (HV; n=17) by Taqman quantitative real-time (qRT)–PCR). $***p < 0.001$, HV vs. MDS. **b** Analysis of ERFE mRNA levels in World Health Organization (WHO) categories of MDS. The data set MDS2 (subclass of GSE58831), consisting of HV (n=17), MDS-SLD (n=13), MDS-MLD (n=27), MDS-RS-MLD (n=22), MDS-EB-1 (n=14) and MDS-EB-2 (n=28), was used for this analysis. Results are expressed as dot plots. Horizontal bars indicate the mean value for each group. $**p < 0.01$, HV vs. MDS-RS-MLD. $***p < 0.001$, HV vs. MDS. Data was analyzed by a one-way ANOVA test (the expression of ERFE mRNA in MDS vs. HV). **c** The level of erythropoietin (EPO) receptor (EPO-R) mRNA in patients with MDS (n=104) as compared with that in HV (n=17). $*p < 0.05$, HV vs. MDS. **d** Analysis of EPO-R mRNA in WHO categories for MDS. $**p <$ 0.01, HV vs. MDS-RS-MLD. $***p < 0.001$, HV vs. MDS. Data was analyzed by a one-way ANOVA test.

Fig. 3 Correlation matrix of different hematological parameters. Scatter plots of all pairwise combinations of the variables: serum ferritin, hemoglobin (Hb), erythroferrone (ERFE) and erythropoietin (EPO) receptor (EPO-R) in BM CD34+ cells are given below the diagonal. The plots are arranged so that all plots in a row share a common Y-axis, whereas all plots in a column share a common X-axis. The names of the X- and Y-axes are shown in the gray boxes in bold letters at the top of the column and right of the row, respectively. The significant respective Spearman rank correlation coefficients are given as overlay in the scatter plot. The correlations were statistically significant: *$p < 0.05$, **$p < 0.01$.

Fig. 4 Production of ERFE protein and screening for its effector cells. a A diagram showing the production of ERFE from HEK293T cells after transfection of an ERFE plasmid. **b** The effect of ERFE-containing conditioned medium (CM; ERFE CM) on HuH7 and HepG2 cell lines. The expression of hepcidin mRNA was examined by SYBR® Green quantitative real-time (qRT)-PCR. *$p < 0.05$ vs. control CM.

Fig. 5 Differentiation of K562 into dysplastic erythroid cells and effects of CM on HepG2. Morphological changes of K562 cells 0 - 4 days after 1 mM SB treatment. **b** Flow cytometric analysis of SB-treated K562 cells using anti-CD235a (glycophorin A)-PE, anti–EPO-R-phycoerythrin (PE) and anti–CD71-fluorescein isothiocyanate (FITC). **c** The effect of supernatant derived from K562- and SB-treated K562 cells on HepG2 cells. *$p < 0.05$ vs. expression of hepcidin on day 0.
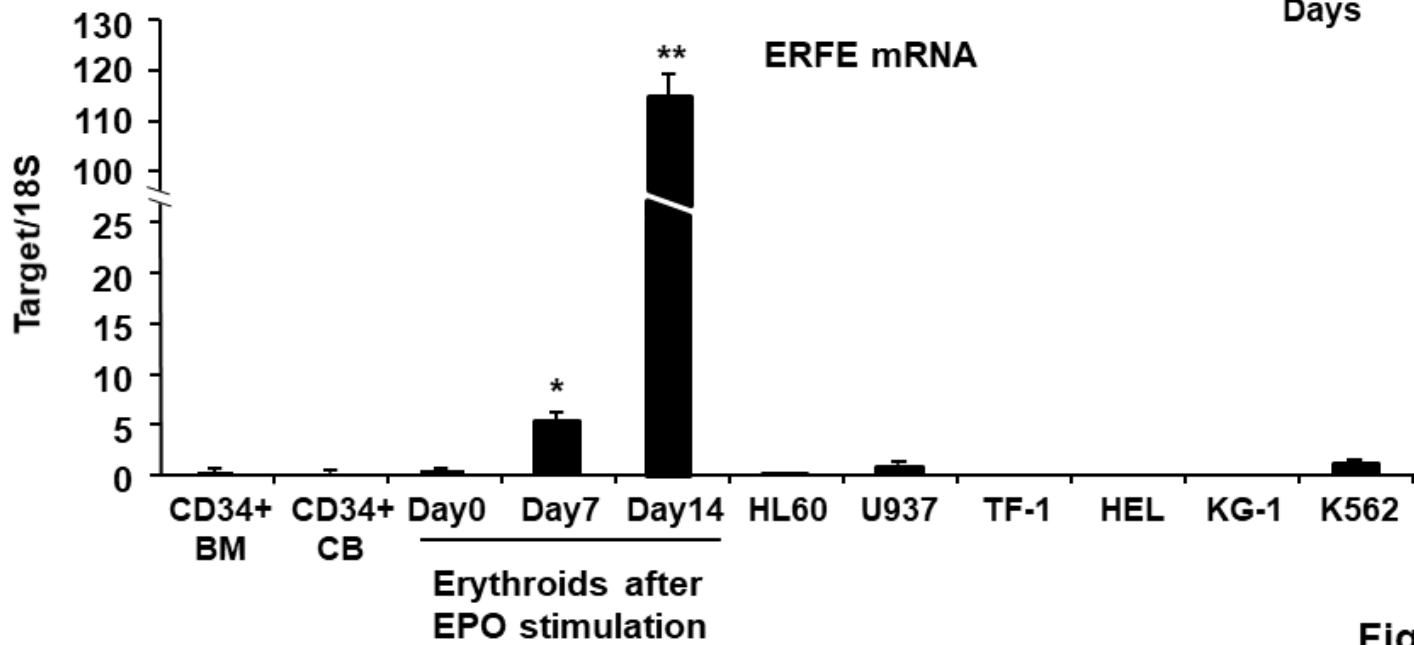
a
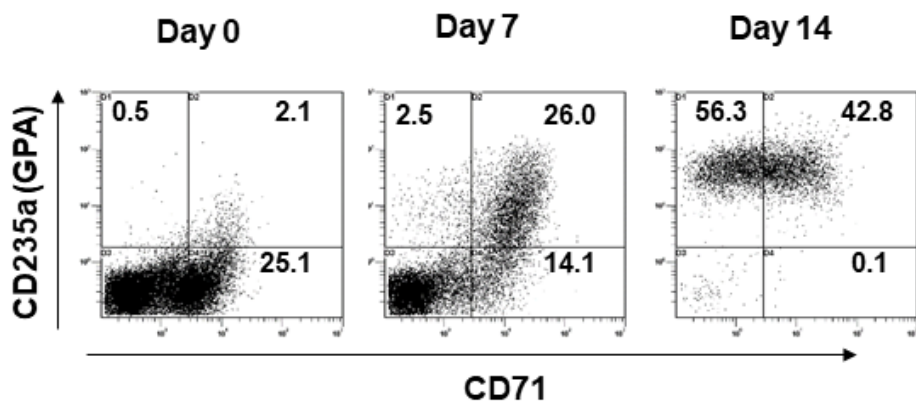
b
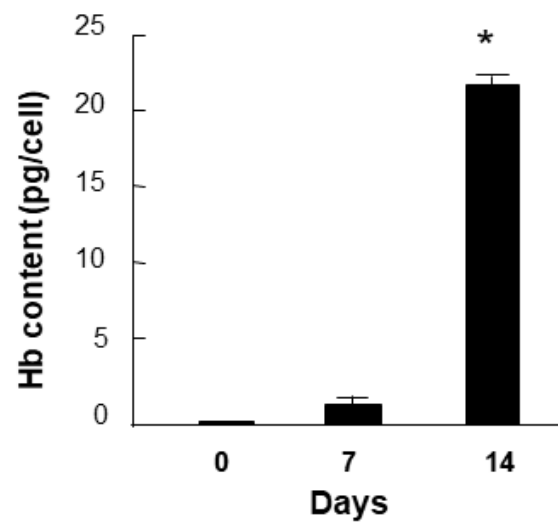
c

Figure 1
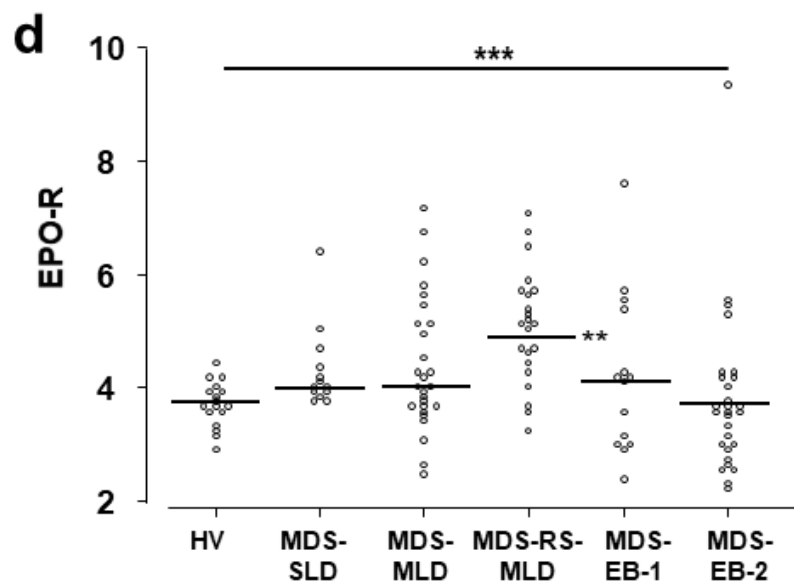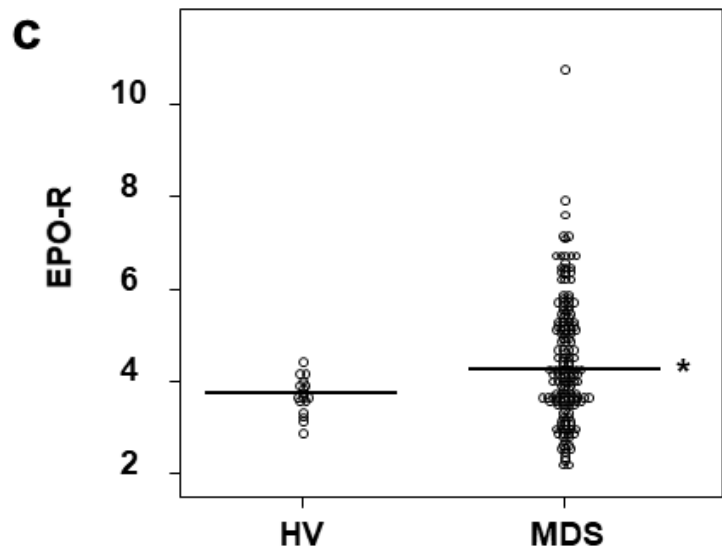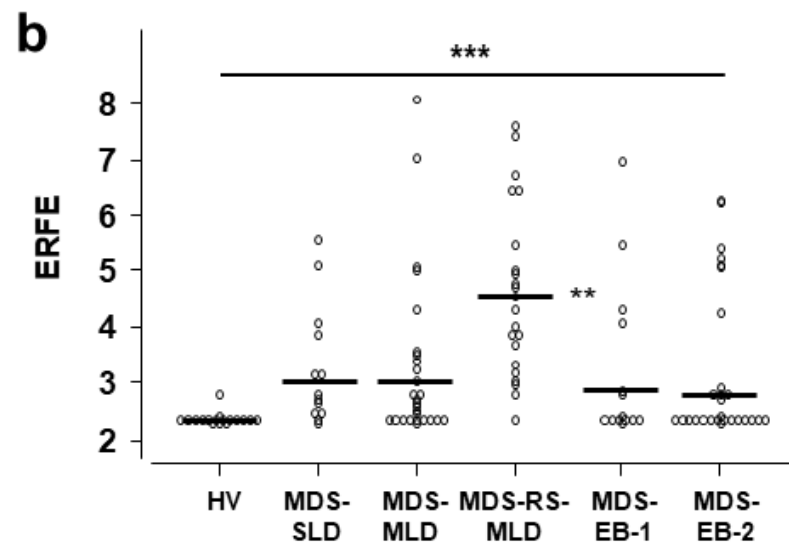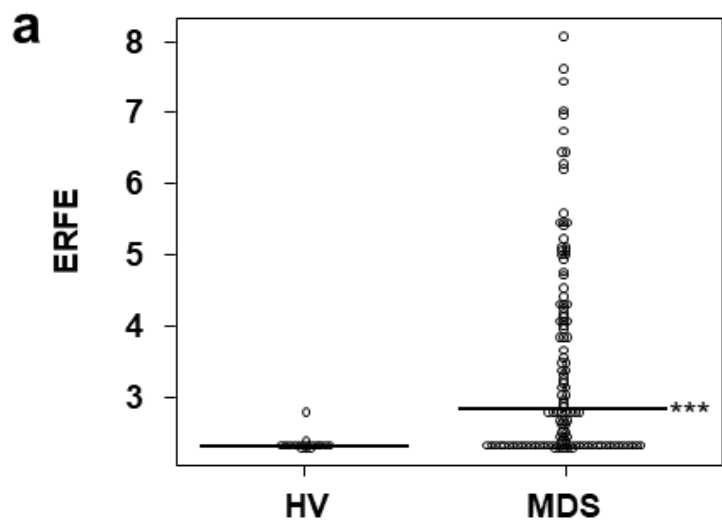
Figure 2

Figure 3

Figure 4

a

Day 0   Day 2   Day 4

b

	Day 0	Day 2	Day 4

CD235a-PE

| 1.8 | 72.9 | 5.4 | 72.4 | 3.8 | 93.0 |
| 4.5 | 23.8 | 4.5 | 17.6 | 0.9 | 2.3 |

EPOR-PE

| 3.9 | 89.9 | 9.6 | 66.7 | 4.0 | 86.2 |
| 2.1 | 4.1 | 7.5 | 16.3 | 1.6 | 8.2 |

CD71-FITC

c

Hepcidin / 18S

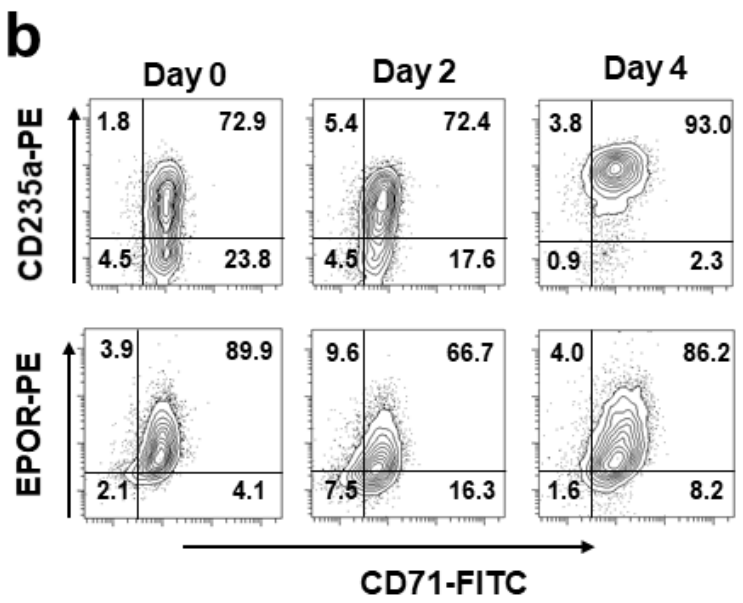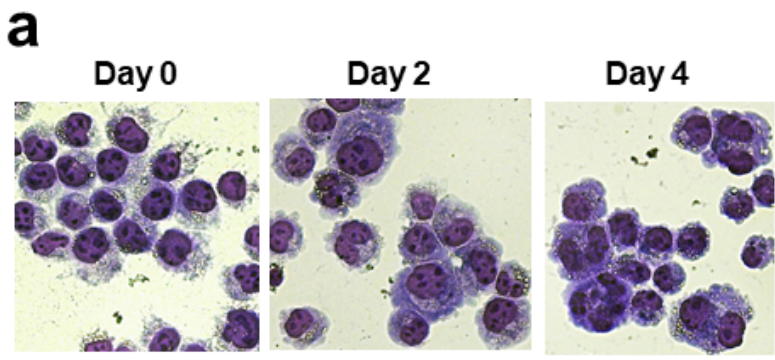| SB	-	+	+
EPO	-	-	+
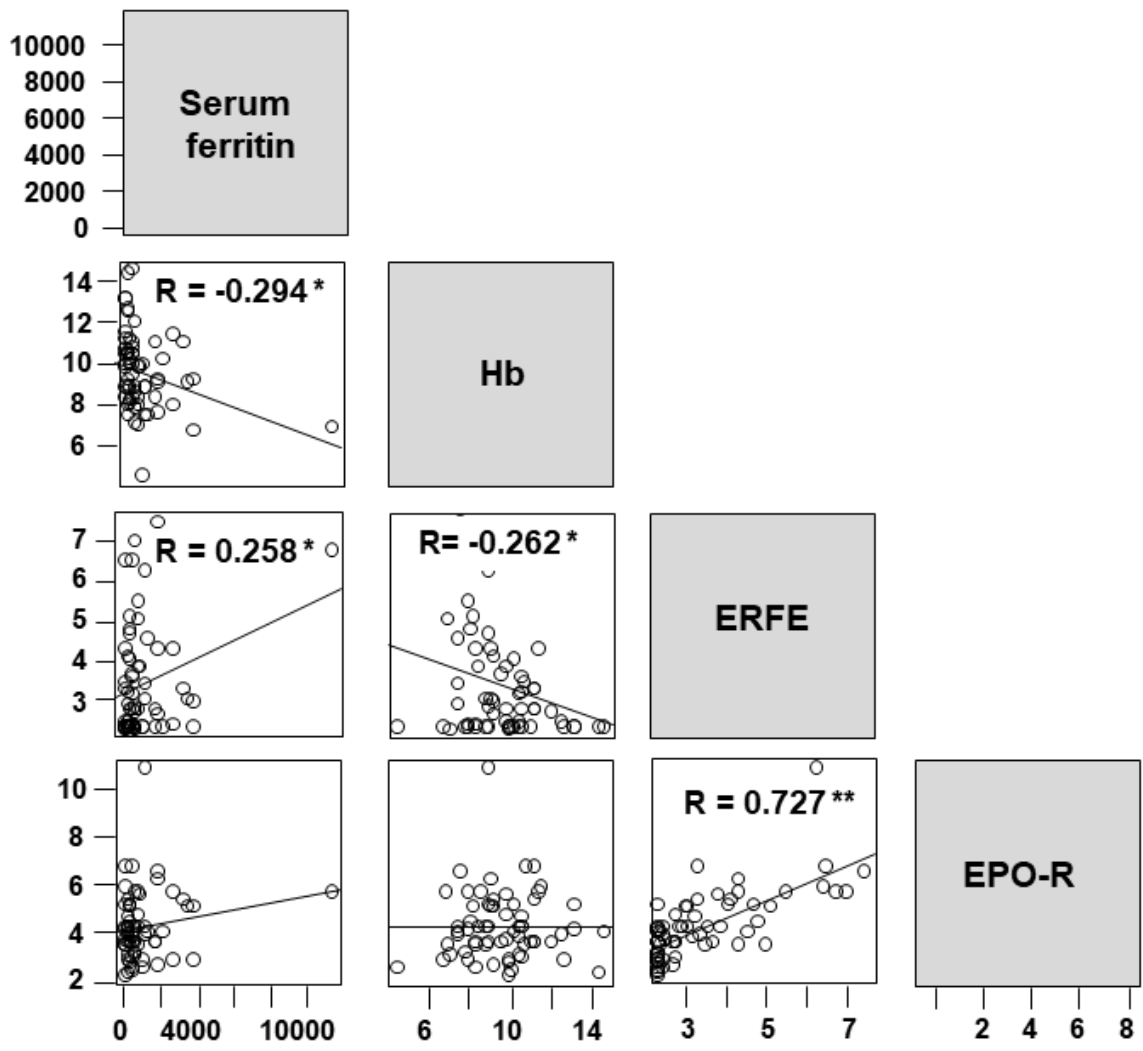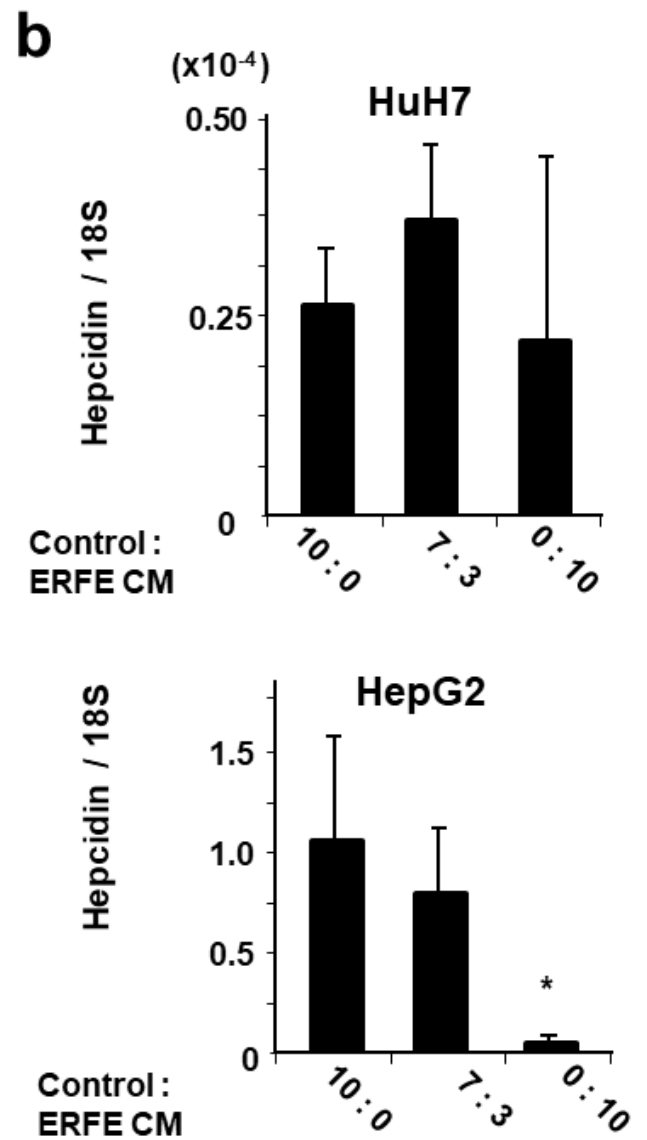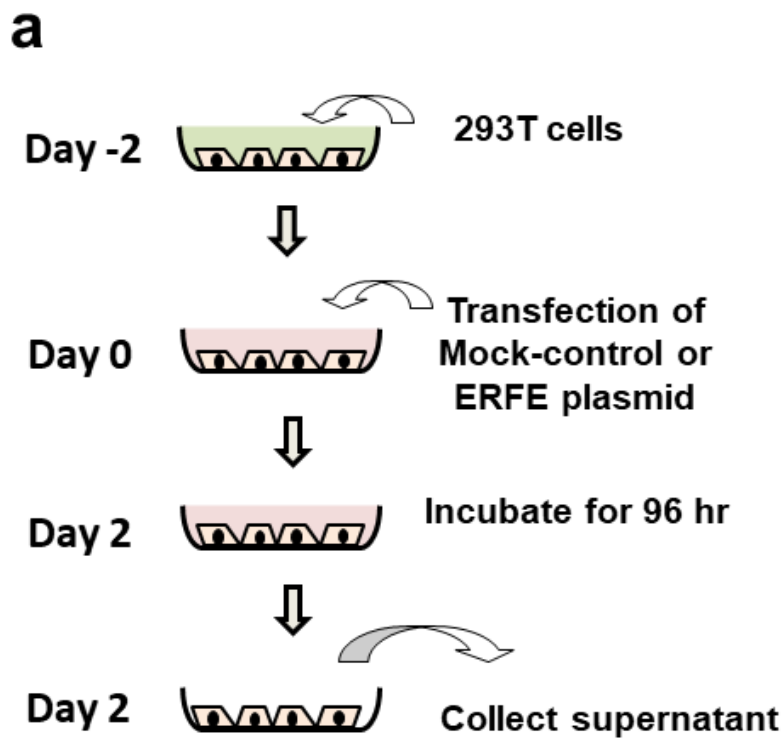
Day 0   Day 4
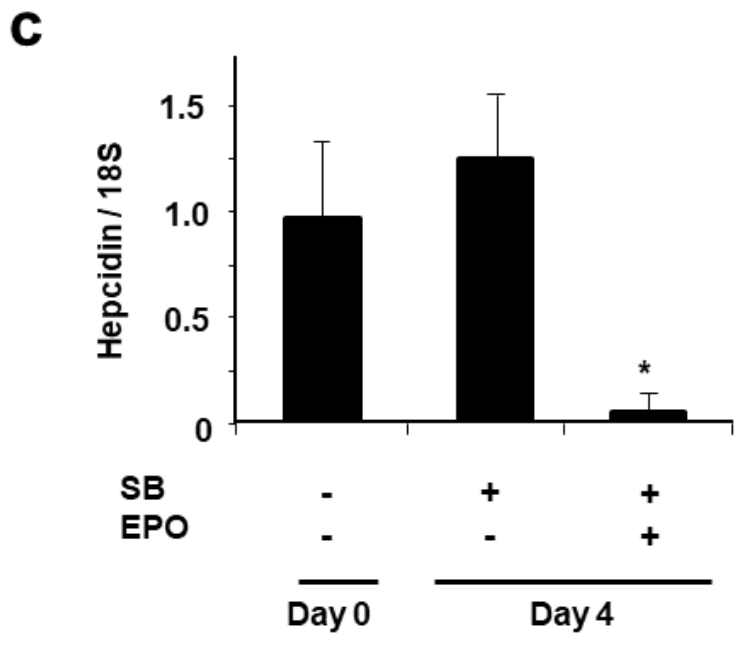
Figure 5

Table 1. Multiple regression analysis of relationship between gene mutations and ERFE mRNA expression

	Estimate	Std. Error	t value	*P* value
(Intercept)	3.4039	0.178	19.1131	0.00000
BCOR	1.3458	0.8474	1.5881	0.11523
CDKN2A	-3.2715	1.9805	-1.651	0.10152
CUX1	0.6552	0.8371	0.7827	0.43552
DNMT3A	-0.6964	0.4411	-1.5788	0.11736
EP300	-0.8662	1.4117	-0.6136	0.54079
ETV6	-1.0964	1.4117	-0.7766	0.43908
EZH2	-0.0251	0.5519	-0.0455	0.96372
FLT3	0.4656	1.0061	0.4628	0.64444
GATA2	-2.0233	1.4257	-1.4191	0.15879
IDH1	-1.0965	1.4117	-0.7767	0.43906
IDH2	-0.8495	0.8659	-0.981	0.32879
JAK2	0.272	0.6668	0.408	0.68409
KDM6A	2.1563	1.4117	1.5274	0.12963
KRAS	1.4925	1.4117	1.0572	0.29279
SF3B1	0.9761	0.3021	3.2308	0.00164
SH2B3	-1.0965	1.4117	-0.7767	0.43906
STAG2	-1.0127	0.5434	-1.8635	0.06515

The data set MDS1 (subclass of GSE58831) consisting of HV (n=17), MDS-SLD (n=13), MDS-MLD (n=27), MDS-RS-MLD (n=22), MDS-RS-SLD (n=20), MDS with isolated del(5q) (n=6), MDS-EB-1 (n=14) and MDS-EB-2 (n=28) were used for these analyses. The left column indicates gene symbols used in this analysis.

Table 2. Stepwise regression analysis of relationship between ERFE mRNA and other iron metabolism–related genes

|	Estimate	Std. Error	t value	*P* value
(Intercept)	7.110364	1.920539	3.702274	0.0002884711
ALAS2	0.165188	0.026700	6.186894	0.0000000044
EPO-R	0.702592	0.058391	12.032624	0.0000000000
NFS1	-0.684728	0.316957	-2.160321	0.0321480900
PCBP2	-0.350947	0.150933	-2.325187	0.0212434000
TFR2	-0.436569	0.173913	-2.510276	0.0129979700

The MDS2 data set (subclass of GSE58831) consisting of HV (n=17), MDS-SLD (n=13), MDS-MLD (n=27), MDS-RS-MLD (n=22), MDS-EB-1 (n=14) and MDS-EB-2 (n=28) was used. The left column indicates the gene symbol used in this analysis.

Supplementary Table 1. Primer set IDs for genes examined using Taqman quantitative real time PCR

Gene name (Gene symbol)	Taqman Assays ID
GDF15	Hs00171132_m1
TWSG1	Hs00221028_m1
ERFE	Hs00937727_m1
Human ribosomal protein S18 (*18S rRNA*)	Hs9999901_s1

Supplementary Table 2. Real-time SYBR® Green PCR, primer set IDs

| Gene symbol	Primer set IDs
ERFE (FAM132B)	PPH58367A
HAMP (Hepcidin)	PPH06152A
GDF15	PPH01935C
18S rRNA	PPH05666E
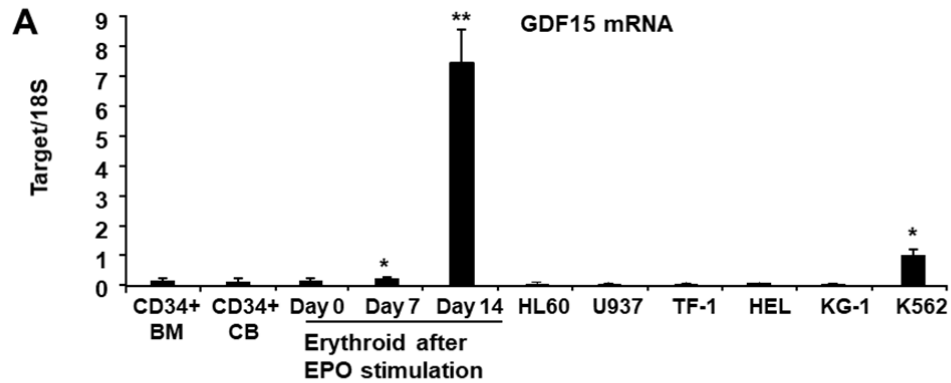
A GDF15 mRNA

Supplementary Fig. 1 Analysis of the expression of GDF15 mRNA in erythroid cells and leukemic cell lines. Expression levels of GDF15 mRNA were examined by Taqman quantitative real-time (qRT)-PCR. Results are expressed as means ± standard deviation (SD). Data represent three independent experiments, each done in triplicate. $*p < 0.05$, $**p < 0.01$ vs. day 0 in the respective group.

TWSG1 mRNA
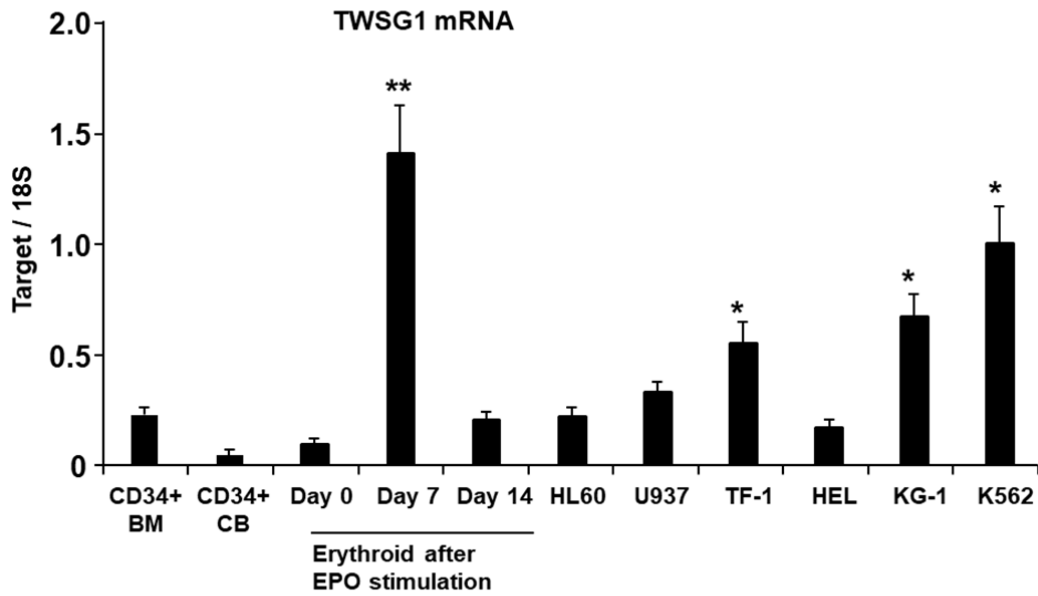
Supplementary Figure 2

Supplementary Fig. 2 Analysis of the expression of TWSG1 in erythroid cells and leukemic cell lines. Expression levels of TWSG1 was examined by Taqman quantitative real-time (qRT)-PCR. Results are expressed as means ± standard deviation (SD). Data represent three independent experiments, each done in triplicate. $*p < 0.05$, $**p < 0.01$ vs. day 0 in the respective group.
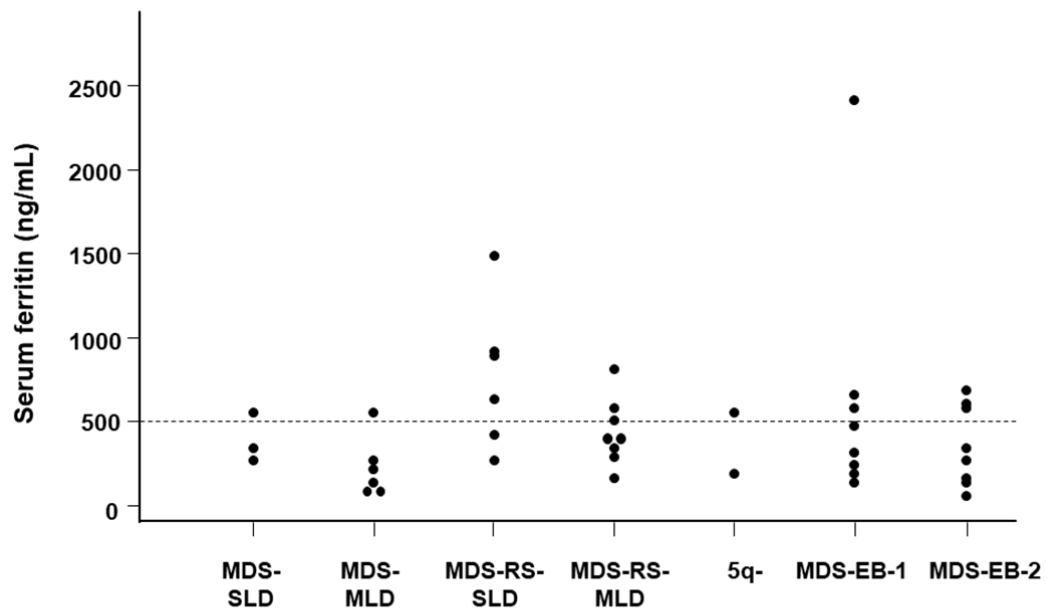
Supplementary Fig. 3 Serum ferritin levels in transfusion-independent myelodysplastic syndrome. The y-axis indicates the serum ferritin level. The x-axis indicates each World Health Organization category. From data set MDS2, patients with non-transfusion–dependent myelodysplastic syndrome were selected by EZR software.